FACULTY OF INFORMATION TECHNOLOGY AND ELECTRICAL ENGINEERING

DEGREE PROGRAMME IN WIRELESS COMMUNICATIONS ENGINEERING

MASTER'S THESIS

JOINT ENERGY HARVESTING TIME ALLOCATION AND BEAMFORMING IN TWO-WAY RELAYING NETWORK

Author	Ngo Trung Kien
Supervisor	Prof. Markku Juntti
Technical Supervisor	Dr. Quang-Doanh Vu
Second Examiner	Dr. Quang-Doanh Vu

February, 2019

Ngo K. (2019) Joint Energy Harvesting Time Allocation and Beamforming in Two-Way Relaying Network. University of Oulu, Faculty of Information Technology and Electrical Engineering, Degree Programme in Wireless Communications Engineering. Master's Thesis, 37 p.

ABSTRACT

A two-way relaying system with amplify-and-forward technique, where relay stations (RSs) acquire the energy from transmission signal and interferences, is considered. The RSs use the energy to amplify the signal received from the transmitter and forward it to the receiver. Particularly, energy harvesting (EH) and time switching (TS) are deployed. Based on the TS architecture, we divide transmission time into two time slots, which are EH phase and information transmission (IT) phase. In the EH phase, the RSs harvest the energy from the received radio frequency (RF) signal. In the IT phase, the RSs process and forward the transmission signal to the destination by energy harvesting during the EH phase. From such a transmission scheme, we investigate the optimal time ratio of the EH and IT phase as well as the beamforming at RSs in order to acquire the sum rate maximization. Since the sum-rate maximization problem is nonconvex, we develop an iterative algorithm based on the majorization-minimization (MM) technique to solve the problem. Furthermore, we deployed two schemes to overcome the self-interference to see the efficiency of each scheme related to sum-rate performance. The results show that power transmission and a number of relay station have a major impact on the sum rate performance of the two-way relay system.

Keywords: two-way relaying, energy harvesting, wireless power transfer, sum rate maximization, majorization-minimization, information transmission, time switching.

TABLE OF CONTENTS

FOREWORD

The focus of this research is to study the energy harvesting time allocation between two phases in two-way relaying networks. This thesis was carried out at Centre for Wireless Communications (CWC) at University of Oulu.

A special thanks to my supervisor Dr. Quang-Doanh Vu who always very supportive and genuinely interested during the time that I am preparing for my thesis. I would like to thank Prof. Markku Juntti for giving me the opportunity to do my thesis at CWC.

Furthermore, I would also like to thank Mr. Kien-Giang Nguyen who is spending countless time helped me understand the new theory and simulation tools that support me completed this thesis.

I would like to thank all my teachers at University of Oulu for priceless knowledge. I also would like to thank classmates, colleagues, and friends for help and a great environment to study at Univerisity.

Special thanks to my parents, brother, sisters who supported me all the time that give me a strength to go through all the hardship during this journey.

Oulu, January 10, 2019

Kien Ngo Trung

LIST OF ABBREVIATIONS AND SYMBOLS

AF	Amplified-and-Forward
CF	Compress-and-Forward
CSI	Channel State Information
DF	Decode-and-Forward
DoC	Difference-Of-Convex
DTV	Digital television
EF	Estimate-and-Forward
EH	Energy Harvesting
GSM	Global System for Mobile communications
ID	Information Decoding
IoT	Internet-of-Things
IT	Information Transmission
MABC	Multiple Access Broadcast
MM	Majorization-Minimization
PSR	Power splitting-based relaying
RF	Radio Frequency
RFID	Radio-frequency identification
RS	Relay Station
SWIPT	Simultaneous Wireless Information and Power Transfer
TDBC	Time Division Broadcast
TS	Time Switching
TSR	Time switching-based relaying
WPN	Wireless Power Node
WSN	Wireless Sensor Network

$\boldsymbol{w}$	Beamforming vector
h_{kl}	Channel coefficient between user k and relay l
$\boldsymbol{h}_k$	Channel vector between user k and relays
w_l	The processing coefficient used at relay l
$\tilde{y}_k$	The signal received at user k
$\hat{y}_k$	The signal after suppression at user k
γ_k	Signal-to-interference-plus-noise ratio (SINR) at user k
τ	Fraction of time block the relays use for harvesting energy
P_k	The radiated power at user k
$E_l(\tau)$	The total energy harvested at relay l
L	Number of relay station
$\bar{P}_l$	The maximum harvested power
a_l and b_l	Constant parameters related to EH circuit modules
y_l	Signal received at relay l
s_k	Normalized symbol transmitted by user k
n_l	Additional white Gaussian noises (AWGN).

$\epsilon_l(w)$	Amplifier efficiency at relay l
$\hat{\epsilon}_l$	Maximum efficiency by the amplifier
$\hat{P}_l$	Maximum power outputted by the amplifier
$P_l^{\text{amp}}(\mathbf{w})$	The power consumed by the amplifier at relay l
E_l^c	Constant circuit energy consumption at relay l
$R_k(\mathbf{w}, \tau)$	Data rate transmitted by user k
$\| \quad \|_2$	The ℓ_2 norm
$\| \quad \|$	The absolute value
$\mathbb{C}^{m \times n}$	The space of complex matrices of dimensions given in superscript
$\boldsymbol{I}_n$	The $n \times n$ identity matrix
$CN(0, a)$	A complex Gaussian random variable with zero mean and variance a
$\Re(\cdot)$	A real part of the argument
$\boldsymbol{X}^H$	Hermitian transpose of X
$\boldsymbol{X}^T$	Normal transpose of X
$\text{diag}(\boldsymbol{x})$	The diagonal matrix constructed from element of x
$\odot$	The Schur-Hadamard (element-wise) multiplication

1 INTRODUCTION

1.1 Motivation

In the future, wireless access will not only help to connect people but also bring benefits to anything that connected. For example, internet of things (IoT) can create new operation and business opportunities. We are already at the beginning of a transition into a fully connected networked society that will provide full connectivity to help people reading information and sharing of data anywhere and anytime [2][3].

Traditionally, all wireless networks devices and user devices are powered by replaceable batteries with a limited lifetime. In recent year, energy harvesting (EH) technology has become an appealing solution to that problem. There are two main groups of energy sources to harvest, namely,

- Ambient energy sources, e.g., solar, wind energy and radio frequency (RF) energy
- Human power, e.g., breathing, finger movement.

In outdoor environments, the most accessible and often the most advantages technology are the ambient ones, for example, solar and wind energy. However, harvesting natural energy can face technical challenges because of the instability of the natural environment. On the other hand, RF energy can provide a sustainable and stable power supply, is more promising in developing different application and services for the future.

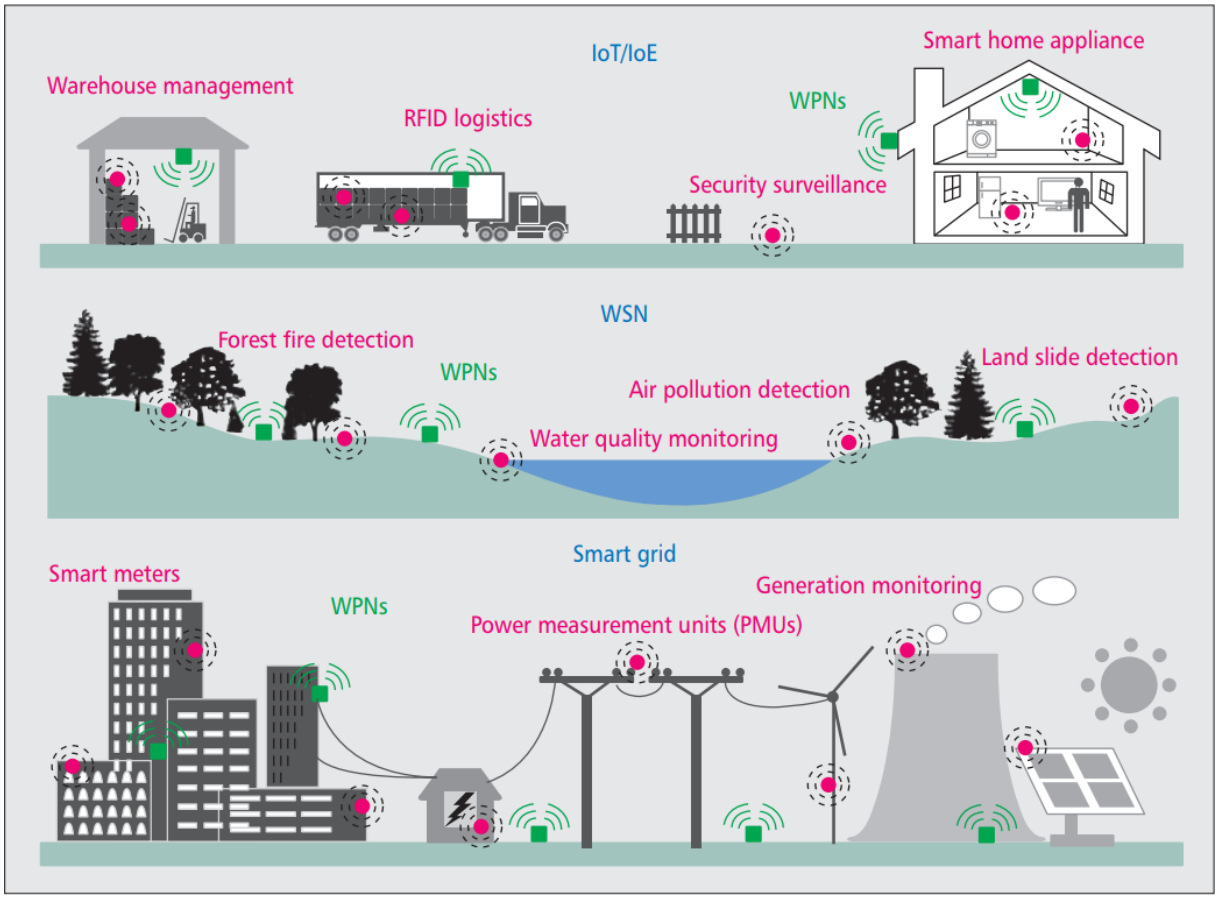

Figure 1. Applications of wireless communication networks with Energy Harvesting [1].

For instance, the recent trends in IoT and smart grid, etc., are an emerging concept of network connectivity anytime and anywhere for billions of nodes [1]. The application of energy harvesting is illustrated in Figure 1 for IoT, wireless sensor network (WSN), and smart grid. All the green nodes can be described as a wireless power node (WPN) will transfer power supply to all other red nodes which can be sensors or nearby wireless equipment.

However, the IoT network system, with a massive number of devices, is facing with a lot of significant problems to achieve all the potential of this system. For example, in the future, countless nodes will be hidden in the walls or deployed in remote or hazardous. The battery life expectancy is usually from two to five years depending on the power consumption of the node with current battery technology. That has become major problems for any IoT system and we need optimizing energy constrained is accessible in every problem need to solve in order to increase the battery life expectancy.

Radio frequency energy transfer and harvesting techniques have recently become alternative methods to acquire energy support for next-generation wireless networks. There are plenty of benefits of this emerging technology such as enables proactive support energy for wireless devices. It can be used advantageously in supporting applications with quality-of-service requirements [2]. However, there are required substantial research in this area in order to achieve the full potential of energy harvesting technology, such as system architecture, RF energy harvesting techniques, and existing applications.

Relay network can be applied in various harvesting energy applications, that needs to have more attentions from the research community. Notably, the next generation network requires the coverage area in the smaller cell such as in the 5G network. The research in the relay network might make a significant contribution in the near future by increasing the efficiency and reducing the cost implement for the real system. In this thesis, the main focus is the RF energy harvesting problem in the two-way relay network.

1.2 Summary of Contributions

In this thesis, the main contribution is described in Chapter 4 and Chapter 5. The thesis shows the significantly different between a non-linear model and a linear model in harvesting energy system. The main contributions of this thesis can be summarized as follows. The main point of this thesis is optimizing time ratio and beamforming at relays for maximizing sum rate. *The relation between power transmission, the number of relays and sum-rate maximization performance.* The thesis deployed two schemes to overcome the self-interference issue.

1.3 Outline of thesis

The rest of this thesis is organized as follows: in Chapter 2, literature review discusses some of the necessary theoretical background and the most current development in the energy harvesting area. In Chapter 3, system model and problem formulation provide the full thesis carried out, network scenario, a system model that will be used in order to formulate the problem. Then, the

thesis provides all detail about transformation and expression to transform the problem. We also evaluate several scenarios to measure the influence of each element in the problem formula. In Chapter 4, we discuss proposed algorithm presents the method for solving the nonconvex problem formulated. After that, in Chapter 5, there are two schemes proposed for this section that overcoming the overhead disadvantage of self-interference. In Chapter 6**,** this part provides several numerical results based on all the scenario that discuss in the previous chapter, and analytical results of that. The inside research problem being investigated and present ideas for future development related to harvesting energy challenges in Chapter 7. Finally, we present our conclusion provides a summary for this thesis in Chapter 8.

2 LITERATURE REVIEW

In this section, we review the literature on RF energy harvesting architecture, simultaneous wireless information and power transfer and two-way scenarios with the time switching architecture.

Wireless power transfer, which is related to transmitting information wirelessly, has become an attractive topic to researchers in a long time. Traditionally, free-space beaming and antennas with large apertures are used to overcome propagation loss for massive power transfer. The power transmission area by radio waves is identified with emphasis upon the free-space microwave power transmission era beginning in 1958. For example, in the 1960s, the authors in [2] demonstrated a small experiment energy harvesting at 2.45 GHz. For transmit power of 2.7 GW, the power transfer efficiency is estimated to be 45% over a transfer distance of 36 000 km.

Technology development in RF energy harvesting circuit, low power transfer for powering mobile terminals in wireless communication systems began to attract increasing attention. The proposed network architecture for RF charging stations and harvest-then-transmit protocol is introduced for power transfer in a wireless broadcast system. Furthermore, various modern beamforming techniques are employed to improve power transfer efficiency for mobile applications. The dual use of RF signals recently brings more advantage for delivering energy as well as for transporting information. Simultaneous wireless information and power transfer (SWIPT) is proposed for later development [2]-[7].

SWIPT provides the advantage of delivering a control label and efficient delivery wireless information and energy concurrently. This system provides a low-cost option for sustainable operations of wireless systems without hardware modification on the transmitter side [5][6]. However, recent research has required that optimizing wireless information and energy transfer need to take into account the optimization of the system performance. That brings trade-off on the design of a wireless system. Hence, the amount of transmitted information and transferred energy cannot be generally maximized at the same time. Therefore, the system performance raises the demand for redesign of existing wireless networks.

RF energy harvesting has multiple applications in various forms, such as wireless sensor networks, wireless body networks, and wireless charging systems. The radio frequency from 3 kHz to 300 GHz is used as a vehicle to transfer information with energy in the form of electromagnetic radiation [2]. RF energy transfer and harvesting are one of the wireless energy transfer techniques. They are currently some near-field power transition. However, they are not suitable for mobile and remote charging in far-field like in the telecommunication system.

In contrast, RF energy transfer proving the benefits to overcome that disadvantage. As the radiative electromagnetic wave cannot retract upon the antenna that generates it by capacitive or inductive coupling at above $\lambda/(2\pi)$, RF energy transfer can be regarded as a far-field energy transfer technique. Hence, the RF signal is the perfect design for powering a massive number of node/devices distributed in a coverage area. The signal strength of far-field RF transmission slightly attenuated according to the environment and the distance between two transceivers, specifically, 20 dB per decade of the distance. The RF energy transfer technique has clear advantages in effective energy transfer distance. However, there are still challenging to develop

this technology in the existing system, such as low RF to direct current (DC) energy conversion efficiency especially when the harvested RF power is small [2], [5].

2.1 Overview of RF Energy Harvesting Network

In this section, we describe the common architecture of the energy harvesting network and also introduce the well-know RF energy harvesting techniques available at this moment.

2.1.1 RF Energy Harvesting Architecture

The most popular centralized architecture for RF energy harvesting is shown in Figure 2. This architecture contains three major parts: Information gateways, the RF energy sources, and network nodes and devices [2], [8].

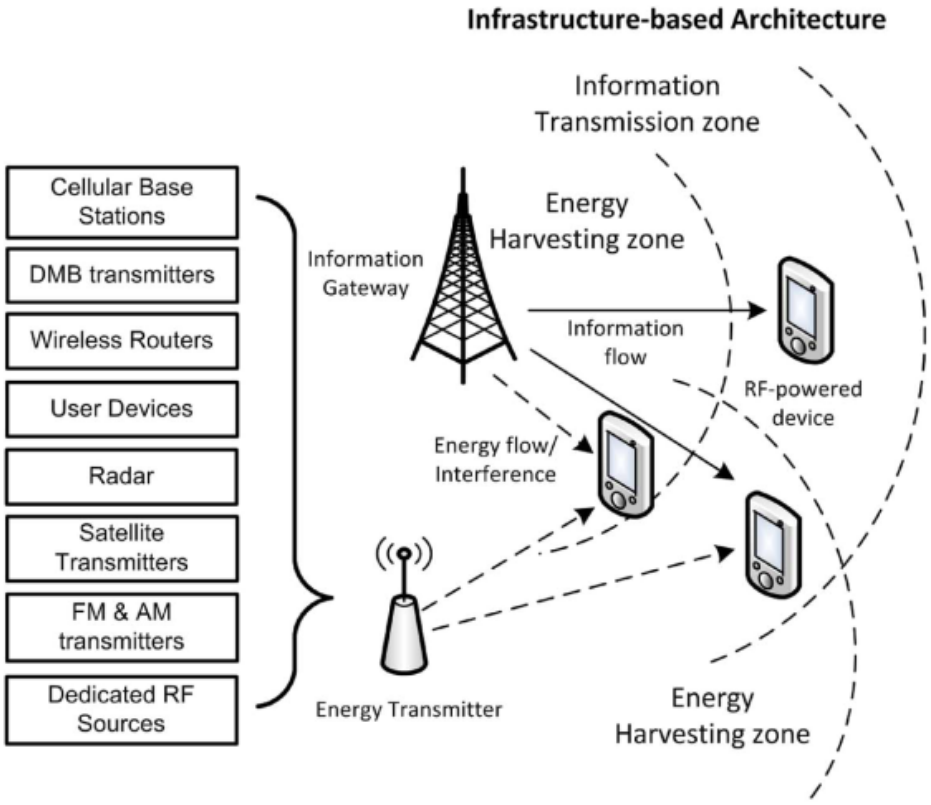

Figure 2. Infrastructure-based Architecture [4].

- The information gateways: known as base stations, wireless routers and relays which have continuous and fixed electric supply
- The RF energy sources: can be dedicated to RF energy transmitters or ambient RF sources which have continuous and fixed electric supply
- The network nodes: All the user equipment that communicates with the information gateways that harvest energy from RF Energy sources to support their operations.

In Figure 2, the solid arrow lines represent information flows and the dashed arrow lines mean energy flows. The information gateway contains the energy harvesting zone and an information transmission zone represented by the dashed curves. The harvesting zone defines as all the nodes in this area can harvest energy from the information gateway. The information

transmission zone defined to help all the node in this area can successfully transmit information from the gateway. The energy harvesting zone is always defined as smaller area than the information transmission zone to ensure the transmission successful of nodes in this area. Energy harvesting is taking into research in different aspect such as spectrum sharing energy cooperation [9]-[12].

2.1.2 RF Energy Harvesting Technique

RF energy harvesting has different characteristics compared to harvesting from other energy sources [4].

- RF sources can provide manageable and constant energy supply over distance for RF energy harvesters.
- The harvested energy can predictable and approximately steady over time with fixed distance in a fixed scenario of RF energy harvesting.
- The distance between RF source and RF energy harvesters is an essential factor that affects the amount of harvested RF energy. Hence, the RF energy harvesters in a different position can have significant variation in harvested RF energy.

The RF sources that can be classified into two categories are dedicated to RF sources and ambient RF sources. Dedicated RF sources can be deployed in the scenario, where the RF harvester's node in the network need stable and predictable energy supply. The dedicated RF sources can use specific frequency or the industrial, scientific and medical radio bands for RF energy transfer. However, deploying the dedicated RF sources will increase the infrastructure and maintenance cost in the network system. Furthermore, the transmission power limited by the regulations in order to limit the danger of the RF radiations. For example, the maximum threshold is 4 W in the 900 MHz band, and the received power must be attenuated to 10 μW at 20 m distance. Therefore, many dedicated RF sources must deployed to meet all requirement for user demand. The RF energy harvesting process with dedicated RF sources is entirely manageable, and it is more suitable to support applications with a Quality-of-Service (QoS) requirement. In theory, the dedicated RF sources might also be user equipment, such as a mobile phone, which is portable and transfer RF energy to other network nodes. Different RF energy transmission schemes for mobile power transmitters to support wireless sensor networks are investigated in many other types of research.

Ambient RF sources refer to the RF transmitters surrounding area, which are not intended for RF energy transfer. This RF energy can be considered as free because this RF transmitter mainly to support another type of communication, such as TV tower and the cellular base station. Therefore, the transmit power of ambient RF sources varies from time to time, from around 106 W for TV tower, to about 10 W for cellular and RFID systems, to roughly 0.1 W for mobile communication devices and Wi-Fi systems [4]. Ambient RF sources can be further divided into two sub-categories static and dynamic ambient RF sources.

- Static ambient RF sources: Static ambient RF sources, such as TV and radio towers, are the transmitters which expected release constant power over time. Even the static ambient RF sources can provide reliable RF energy. However, the static ambient RF sources could be long-term and short-term support due to other main service schedules such as TV and radio case. Typically, the power density of ambient RF sources is small

at different frequency bands. Consequently, a high gain antenna for all frequency bands is required. Furthermore, the antenna must also be designed to support the wideband spectrum. The distribution of ambient RF sources has strong repulsion, and can support the harvester node obtained a higher RF energy harvesting rate.

- Dynamic ambient RF sources: Dynamic ambient RF sources are the RF transmitters that work periodically or use time-varying transmit power, for example, Wi-Fi access point. The RF energy harvesting from the dynamic ambient RF sources must be flexible and inventive to search for energy harvesting opportunities in a specific frequency range. Recently, energy harvesting from dynamic ambient RF sources in a cognitive radio network is proposed to solve the energy crisis in the near future. Generally, a secondary user can harvest RF energy from nearby RF sources, and it can transmit data from that frequency when a sufficiently distance from primary users or when the nearby primary users are idle during that time.

2.1.3 Simultaneous Wireless Information and Power Transfer (SWIPT)

Simultaneous wireless information and power transfer (SWIPT) is designed to save spectrum, like in Figure 3, by transmitting information and energy jointly using the same waveform [5]-[10]. The RF signals always carry energy that we use as a vehicle for transporting information. Since there will be more and more wireless devices, more unwanted signal will be available. The question is how we can make the benefit from unwanted signal power when it becomes more and more critical. SWIPT appears as a state-of-the-art solution for the previous question. SWIPT becomes an exciting new area of research that attracts increasing attention from researchers.

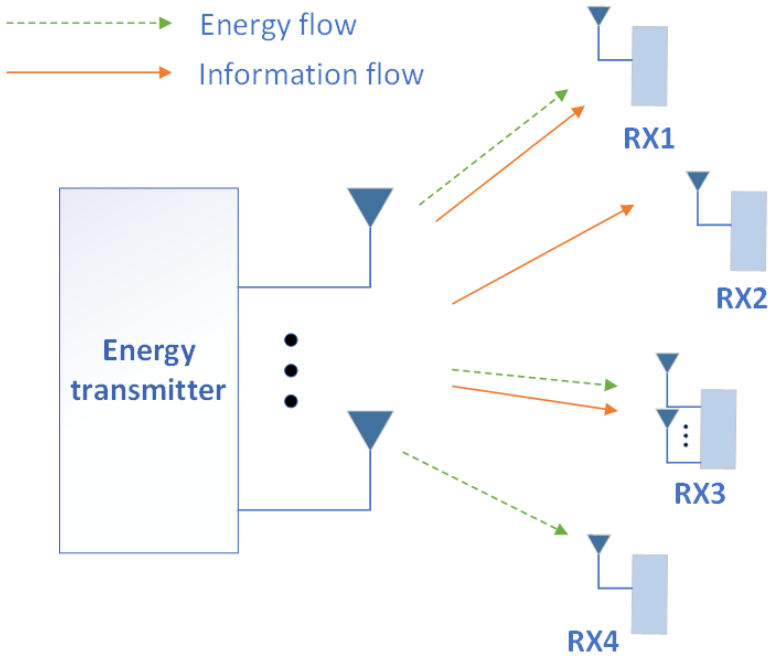

Figure 3. A SWIPT network model.

Any waveform for information transmission also carries energy, which can be harvested by the same or different receivers. However, an efficient SWIPT scheme involves a rate-energy trade-

off in both the transmitter and receiver designs to balance the information decoding (ID) and energy harvesting performance [6], [10]. There is a different kind of SWIPT received structures as shown in Figure 4. There are four types of receiver structures: Separated Receiver, Time Switching Receiver, Power Splitting Receiver, Integrated Receiver.

- Separated Receiver like in Figure 4(a): This architecture supports both in-band and out-of-band RF energy harvesting. In this case, the network node has the separate RF energy harvester and RF transceiver antenna. Hence, the node can simultaneously harvest energy from the energy harvesting link and data communication link.

- Time Switching Receiver like in Figure 4(b): This architecture only supports in-band RF energy harvesting. Each node in the network can harvest RF energy from the same frequency band as that of the data communication link by using time switcher.

- Power Splitting Receiver like in Figure 4(c): This architecture supports out-of-band RF energy harvesting, the network node harvests RF energy from the frequency band different from that used for data communication.

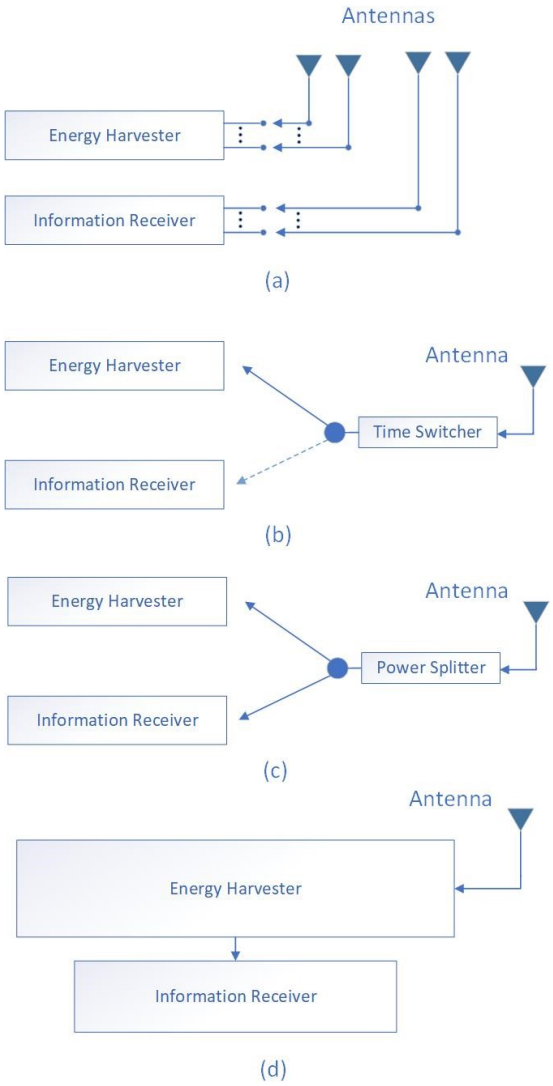

Figure 4. Four kinds of SWIPT receiver structures.

- Integrated Receiver like in Figure 4(d): This architecture is a more theoretical concept that because RF signals can transfer energy as well as information during their transmission. The RF energy harvesting and information reception can be performed from the same RF signal input.

2.1.4 Applications of RF Energy Harvesting

The most widely applied applications of RF energy harvesting is wireless sensor networks. An RF energy harvester scheme can be deployed in a sensor node to provide energy. Various prototype implementations of sensor nodes based on RF energy harvesting are presented in a different experiment. A multi-hop wireless sensor network is also considered for RF energy harvesting development. The actual working concept design an RF-powered transmitter that supports 915 MHz downlink and 2.45 GHz uplink bands in [11]. An average data rate achieved 5 kbps, and the maximum instant data rate is 5 Mbps. The transmitter operated with an input power threshold of −17.1 dBm, and a maximum transmits power of −12.5 dBm [4].

Healthcare and medical applications are also attracted to RF harvesting technology, such as the wireless body network. Low-power medical devices can achieve real-time operation with power supported by dedicated RF sources which are benefiting from RF energy harvesting technology. Furthermore, the devices are less likely to rely on the battery capacity, and it can increase battery lifetime. The design of the RF-powered energy-efficient application featured with a work-on-demand protocol is developing for the next generation of medical equipment. The body device circuit with dual-band operating demonstrated that the antenna obtains gains up to 2.06 dBi and maximum efficiency up to 84%.

Radio-frequency identification (RFID), another RF energy harvesting application that has also caught intensive research is widely used for identification, tracking objectives, and management. Recent developments in technology can enhance the lifetime and range of operation in RFID tags technology. Based on harvesting technology, RFID passive tags can harvest RF energy from other sources instead of depending on the readers and perform communication as active RFID circuits. Therefore, RFID technology has expanded from simple passive tags to smart tags with lately introduced features, for example, sensing and on tag data processing and smart power management [4]. Research progress has enclosed the designs of RFID tags with RF energy harvesting in rectifier, rectenna, charge pump, RF-to-DC converter, and power harvester.

Other than the above popular applications, devices powered by ambient RF energy is an appeal to increasing research attention. For instance, the demonstrates that transmission between two prototype devices powered by ambient RF signals can acquire 1 kbps of an information rate, at the distance of outdoor environment up to 2.5 feet and outdoor environment 1.5 feet. Existing work have also introduced many implementations of devices without battery powered by ambient sources from Wi-Fi, Global System for Mobile communications (GSM) and Digital television (DTV) bands or event ambient mobile electronic devices.

Moreover, RF energy harvesting technology can be used to implement charging capability for a wide variety of low-power user devices such as smart watches, smart headphone, and music players, wireless keyboard and mouse, as most of them spend around micro-watts to milli-watts

range of power. The concept of RF circuit design that enables continuous charging of mobile devices especially in city areas where the density of ambient RF sources is high. That is an excellent example of reducing the power consumption of all electrical devices, which will dramatically increase in the next couple of years.

2.2 Two-Way Relaying Network

Relay networks have recently got more attention from researchers and have been the focus of many studies. In these networks, relay nodes collaborate to establish a communication link between a transmitter and a receiver. There are different relaying schemes that have been presented in the literature. In each case, relays perform different kinds of operations on the received signal before retransmitting it to a destination to preserve or improve the current transmitted power signal.

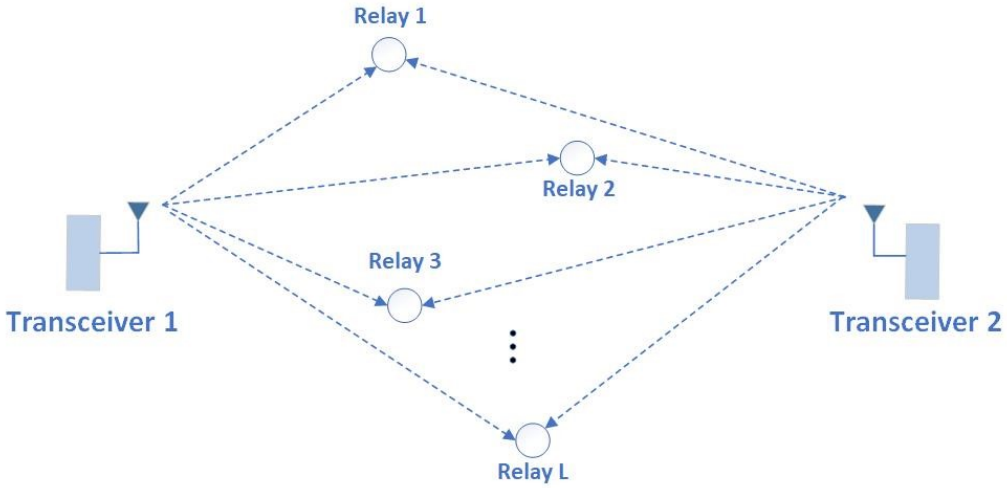

Figure 5. A two-way relay network.

General, two-way relay networks scenario is shown in Figure 5. Two transceivers and multiple RS support in between to help transmitting signal from one to another with none-line-of-sight (NLOS) communication, which can be seen in many existing cases.

2.2.1 Relaying Schemes for Wireless Energy Harvesting

The most popular relaying schemes include the amplify-and-forward (AF) approach, the estimate-and-forward (EF) technique, the decode-and-forward (DF) strategy, and the compress-and-forward (CF) method. In a typical one-way relaying scheme, the communication is established in two steps [16]-[18].

- Firstly, the transmitter sends its signal to the relays. Every RS processes its received signal based on their relaying scheme to produce a new signal.
- After that, the RS transmits a new signal to the receiver. In the AF scheme, each RS amplifies its received signal and forwards that signal to the receiver. There are several advantages of the AF scheme like simplicity in deployment. Therefore their applications and different features have been extensively studied in the literature.

In this thesis, we consider the AF scheme because of its simplicity. The other approaches such as the EF, DF, and CF techniques, require more sophisticated processing power at the RS as

compared to the AF method [16]. That is also not a good option for EH take place in this research at least in this early stage of development.

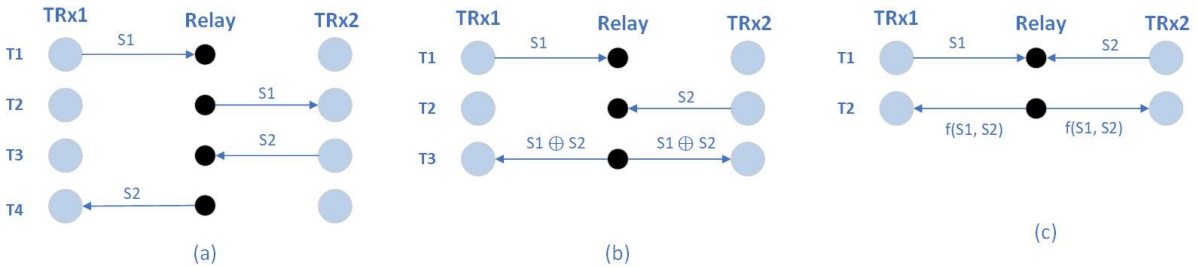

Figure 6. Three different two-way relaying schemes.
(a) Traditional technique. (b) TDBC scheme. (c) MABC scheme

In Figure 6, there are three approaches for deploying two-way relay schemes included: Traditional technique, time division broadcast (TDBC) scheme and multiple access broadcast (MABC).

- Traditional technique approach like in Figure 6(a): The traditional two-way relaying scheme requires four-time slots in order to complete one-time exchange information between two transceivers. This approach is straightforward, and it can avoid interference at the RS and the transceivers. In this case, the topology deploys two successive one-way relaying schemes. However, this traditional scheme is not bandwidth efficient.

- A single-relay TDBC approach like in Figure 6(b): This scheme is introduced in [19]. The author proposes a network coding that is used to reduce the number of time slots from four to three. The relaying scheme requires the RS to combine and decode the signals from both transceivers in the first two time slots. After that, RS sends a broadcasting signal, which is combined with the decoded signals to their destination in the third time slot. Each transceiver can recovery their desire signal by performing an XOR. The performance of the TDBC protocol is provided dramatically higher throughput than that of the traditional four-time slot scheme that is shown in Figure 6(a).

- Finally, MABC schemes like in Figure 6(c): MABC has been presented in [20][21]. Only two timeslots are needed to complete exchanging information between two transceivers. On the first timeslot, both transceivers send their signal to RS, simultaneously. RS will forward the processed version of signals to their destination. Most MABC approaches consider the case of single relay networks.

2.2.2 Relaying Protocols for Wireless Energy Harvesting

A wireless communication system is considered, where the information is transferred from the source node to the destination node through the energy constrained intermediate relay station node. Figure 5 shows the system model for the relaying system. Based on the time switching and the power splitting receiver architectures, there are two relaying protocols to harvest energy from the source RF signal [8]:

i) Time switching-based relaying (TSR) protocol.
ii) Power splitting-based relaying (PSR) protocol.

2.2.2.1 Time switching-based relaying (TSR) protocol

Figure 7 illustrates the critical parameters in the TSR protocol for energy harvesting and information transmission at the RS. In Figure 7(a), T is the block time in which a certain block of information is transmitted from the source node to the destination node and τ is the fraction of the block time in which relay harvests energy from the source signal, where $0 \leq \tau \leq 1$. The remaining block time, $(1-\tau)T$ is used for information transmission, such that half of that, $(1-\tau)T/2$, is used for the source to relay information transmission and the remaining half, $(1-\tau)T/2$, is used for the relay to destination information transmission. All the energy harvested during the energy the harvesting phase is consumed by the relay while forwarding the source signal to the destination. The choice of the time fraction, τ, used for harvesting energy at the relay station, affects the achievable throughput at the destination. The following subsections analyze the best time fraction, τ, to achieve the best maximum rate performance.

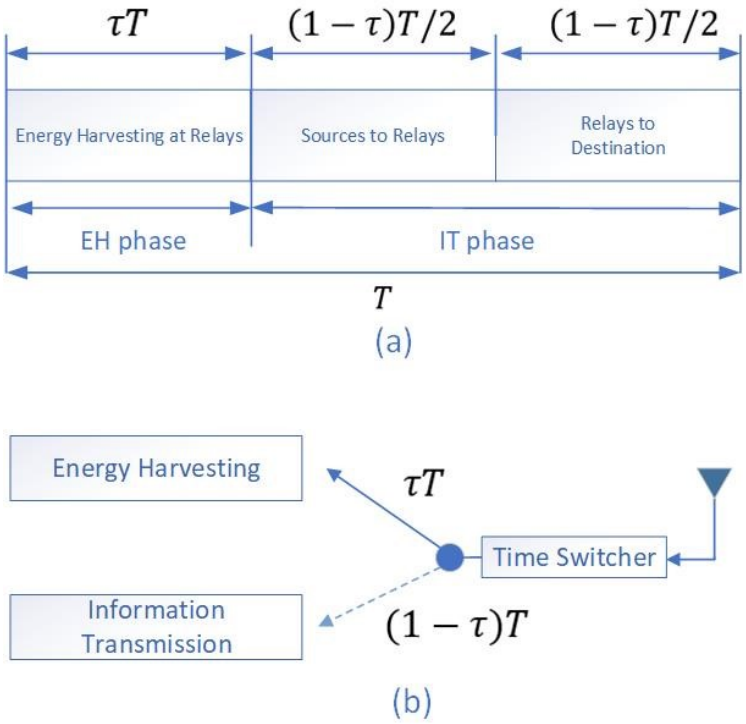

Figure 7 (a) Demonstration of the critical parameters in the TSR protocol for energy harvesting and information processing at the relay. (b) Block diagram of the relay receiver in the TSR protocol.

2.2.2.2 Power splitting-based relaying (PSR) protocol

Figure 8 characterizes the critical parameters in the PSR protocol for energy harvesting and information transmission at the RS. Figure 8(a) shows the communication block diagram employing the PSR protocol for energy harvesting and information processing at the RS. In Figure 8(a), P is the power of the received signal, y_r at the RS and T is the total block time. $T/2$ is used for the source to relay information transmission and the remaining half, $T/2$ is used for the relay to destination information transmission. During the first half of the block time, the fraction of the received signal power, ρP is used for energy harvesting. The remaining received power, $(1-\rho)P$ is used for the source to relay information transmission, where $0 \leq \rho \leq 1$. All

the harvested energy is consumed by the relay while forwarding the source signal to the destination. The choice of the power fraction, ρ, used for harvesting energy at the RS, affects the achievable throughput at the destination.

The diagram for the relay receiver architecture in the PSR protocol is shown in Figure 8(b). The power splitter splits the received signal in $\rho : 1-\rho$ proportion, such that the portion of the received signal, $\sqrt{\rho}y_r$ is sent to the energy harvesting receiver and the remaining signal strength, $\sqrt{(1-\rho)}y_r$ drives to the information receiver. The PSR is a promising protocol, besides TSR, to deployed harvesting energy in two-way relaying network scenarios.

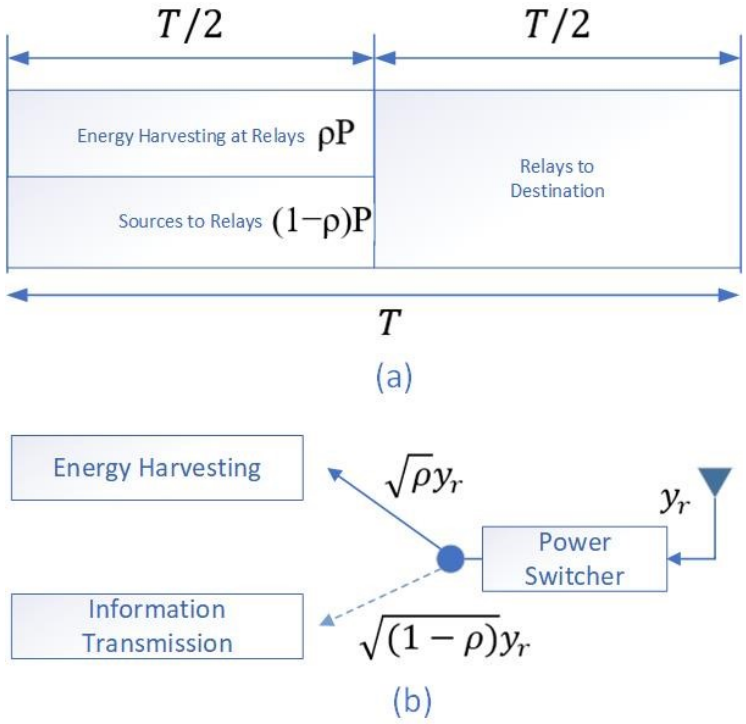

Figure 8 (a) Demonstration of the critical parameters in the PSR protocol for energy harvesting and information processing at the relay. (b) Block diagram of the relay receiver in the PSR protocol.

2.3 Linear and non-linear energy harvesting models

In this section, we focus on the research receiver model for EH in SWIPT systems. In general, a SWIPT system consists of a transmitter of the RF signal. A source sends a signal to the relay station; then it will forward that processed signal to the destination, as well as the reply station harvesting received RF energy. After the signal has been received at the RS, a chain of elements process the signal as follows. The bandpass filter is employed after the receiver antenna performs the required impedance matching and passive filtering, and before the RF signal is passed to the rectifying circuit. The rectifier is a passive electronic device, usually comprising diodes, resistors, and capacitors, that converts the incoming RF power to DC power, which can be stored in the battery storage of the receiver. The rectifier is followed by low-pass filter to eliminate the harmonic frequencies and prepare the power for storage.

The rectifying circuits and their optimization have been a research topic for decades, although recently more attention has been drawn to them, due to their essential role in SWIPT systems. Different configurations of rectifying circuits and an illustration of their efficiency of converting the input RF power to output DC power have been presented. However, we expect that the input-output response of the EH circuit is non-linear, considering that in any possible configuration, the rectifying circuit has at least one non-linear element, such as the diode or diode-connected transistor [22]. The most critical parameter that describes the capability of the rectifying circuit is the RF-to-DC conversion efficiency. In general, the conversion efficiency is defined as the ratio between the output DC power and the input RF power:

The relationship that the efficiency described is shown to be non-linear, due to the non-linear nature of the circuit itself. This non-linearity is observed in all the measurements presented which were performed using practical EH circuits. Similar non-linear behavior also appears when we observe the output DC power concerning the input RF power because they are also connected through the conversion efficiency of the circuit. The problem of modeling the relationship between the input and output power of a rectifier through a general expression has not been reported in the literature. However, an accurate and tractable model is necessary in order to include the effect of practical rectifying circuits on the harvested power at the EH receivers, when working with SWIPT communication systems [22][23].

In practice, the end-to-end wireless power transfer is non-linear and is influenced by the parameters of the practical EH circuits, which are built using at least one non-linear element. Thus, the linear assumption for the conversion efficiency and the EH receiver model does not follow the actual characterization of practical EH circuits in general. Moreover, significant performance losses may occur in SWIPT systems, when the design of a resource allocation algorithm is based on an inaccurate linear EH model. Therefore, the non-linear model needs to be used for harvesting energy in the SWIPT system.

3 SYSTEM MODEL AND PROBLEM FORMULATION

The two-way relay network between point to point connection is recently getting attention from researchers due to the advantages of technology, and it also can consider as crucial key to opening some other technology such as cognitive radio and future connection for an internet of thing. In cooperative communication related to relay station, there are different transmission scheme that can be implemented based on the transmission purpose. There are three main replaying protocols: AF, DF, and CF. In this thesis, we used AF scheme transmission for our own simulation, which is a relay station, after received signal from a transmitter, amplified the signal included noise and interference then forwarded the processed signal to the destination.

The proposed research model is two-way relaying methods with a half-duplex connection. The most typical form two-way relay network, which is two signal antenna transceivers with an amount of number single antenna RSs are used in a simulation model in this paper. We also consider the covariance matrix of channel state information (CSI) of interference known. We optimize the network performance based on the TS architecture in the two-way replaying network. In this case, the ratio between the EH phase and the IT phase has a significant impact on network performance. We find the optimal ratio in order to maximize the sum rate two-way replying network.

In this thesis, we also consider a network consisting of two transceivers and a couple of RSs in between. We assume that there is no direct connection between the two transceivers. In other words, there is only an NLOS connection between two nodes and they communicate with each other through the relay network. Our communication scheme consists of two phases.

In a two-way relaying network, half-duplex communication between two users has become more popular due to its advantage of overcoming the disadvantage of one-way half-duplex. The topology defined two-way relay network contains two single-antenna transceivers and some distributed single-antenna relays [15]. Moreover, the MABC relaying strategy is designed to increase bandwidth efficiency, where only two-time slots are needed to accomplish transmission between two nodes [16]. The general topology that we use in this case is shown in Figure 9.

Figure 9(a) shows the topology where two users are transmitting information through multiple relays where all the relay antenna is designed with time-switching architecture. The relay antenna architecture is shown in Figure 9(b). Finally, the frame structure of the harvest-then-cooperate protocol, where the energy harvesting phase and the information transmission phase will take the whole transmission time slot, is shown in Figure 9(c).

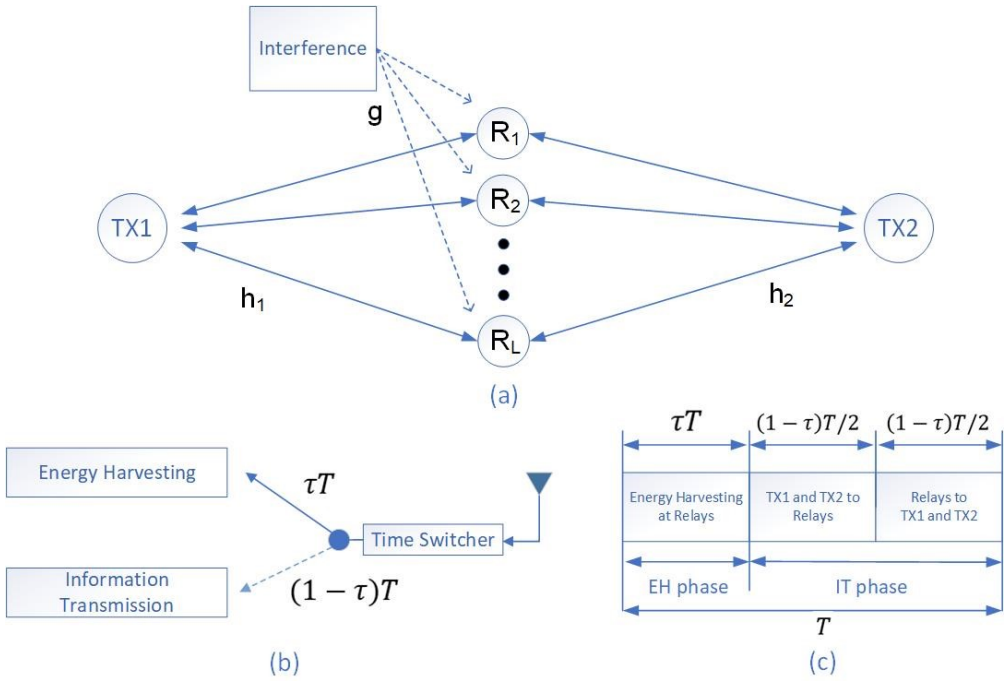

Figure 9. Energy-harvesting based Two-way Relaying network.

Some note for the topology scenario is described as follow:

- In the first time slot, both transceivers transmit their information to the relays station simultaneously. The relays also need to send a broadcast signal to both transceivers to define processed versions that they will transfer in the second time slot.

- In this thesis, we use the AF based MABC relaying protocol. AF is famous for the simple implementation, and smaller delay comparing with other technologies such as DF, and CF. Furthermore, the beamforming technique is also taking into account in the experiment for improving the performance of two-way relaying networks.

We consider a system model where two users communicate with the other via a set of L relays. All nodes are equipped with a single-antenna. Let h_{kl} denote the channel coefficient between user k and relay l. For notational convenience, let us define $\boldsymbol{h}_k \triangleq [h_{k1}, h_{k2},..., h_{kL}]^T$ the channel vector between user k and the relays. We assume that perfect channel state information is known, and the channel reciprocity holds. We also suppose that there is no direct link between users, and the communication between users follows the two-way amplify-and-forward protocol. Furthermore, the relays do not have a constant supplied power and thus they wirelessly receive energy from the users via RF signals. Here time switching protocol is assumed for the simplicity of hardware implementation [4][20]. In particular, each transmission block with time duration T is divided into two portions: the first portion is for energy harvesting at the relay and the second portion is for information transmission. The network coding also take part in this process especially with MABC relaying protocol [21]. The communication details are presented in next section.

3.1 Energy Harvesting:

Let $\tau \in (0,1)$ be the fraction of time block the relays use for harvesting energy. Here we consider a practical non-linear EH model introduced in [22]. Specifically, let us denote by P_k the radiated power at user k .

The total energy harvested at relay l is

$$E_l(\tau) = A_l T \tau \tag{1}$$

where $A_l = \bar{P}_l \left(\frac{1+e(a_l b_l)}{1+e(-a_l(P_1|h_{1l}|^2+P_2|h_{2l}|^2)-b_l)} - 1 \right) / \exp(a_l b_l)$,

$\bar{P}_l$ is the maximum harvested power,

a_l and b_l are parameters related to EH circuit modules, which are constant.

3.2 Information Transmission

The remaining duration of block time, i.e. $(1-\tau)T$, is divided into two equal parts. In the first part, the users transmit information to the relays. In the second part, the relays broadcast the processed signals to the users. In particular, the signal received at relay l is

$$y_l = \sqrt{P_1} h_{1l} s_1 + \sqrt{P_2} h_{2l} s_2 + n_l \tag{2}$$

where s_k is the normalized symbol transmitted by user k ,

$n_l \backsim CN(0, \sigma^2)$ is additional white Gaussian noises (AWGN).

Let $w_l \in \mathbb{C}$ denote the processing coefficient used at relay l . Then the signal received at user k is [15] [24].

$$\begin{aligned} \tilde{y}_k &= \sum_{l=1}^{L} h_{kl} w_l y_l + \tilde{n}_k \\ &= \sqrt{P_k} \mathbf{h}_k^T \mathbf{W} \mathbf{h}_k s_k + \sqrt{P_{\bar{k}}} \mathbf{h}_k^T \mathbf{W} \mathbf{h}_{\bar{k}} s_{\bar{k}} + \mathbf{h}_k^T \mathbf{W} \mathbf{n}_R + \tilde{n}_k \end{aligned} \tag{3}$$

where $\tilde{n}_k \backsim CN(0, \sigma_k^2)$ is AWGN,

$\boldsymbol{w} \triangleq [w_1, w_2, \ldots, w_L]^T \in \mathbb{C}^{L \times 1}$,

$\boldsymbol{W} \triangleq \mathrm{diag}(w)$

$\boldsymbol{n}_{\mathrm{R}} \triangleq [n_1, n_2, \ldots, n_L]^T$; $\bar{k} \in \{1,2\}$ and $k \neq \bar{k}$.

We assume that self-interference terms are correctly suppressed at the users. The signal after suppression at user k is

$$\begin{aligned} \hat{y}_k &= \tilde{y}_k - \sqrt{P_k} \mathbf{h}_k^T \mathbf{W} \mathbf{h}_k s_k \\ &= \sqrt{P_{\bar{k}}} \mathbf{h}_k^T \mathbf{W} \mathbf{h}_{\bar{k}} s_{\bar{k}} + \mathbf{h}_k^T \mathbf{W} \mathbf{n}_R + \tilde{n}_k \end{aligned} \tag{4}$$

User k decodes information from $\hat{y}_k$. Thus, the signal-to-interference-plus-noise ratio (SINR) at user k is

$$\gamma_k = \frac{P_{\bar{k}} \left| \mathbf{h}_k^T \mathbf{W} \mathbf{h}_{\bar{k}} \right|^2}{\sigma^2 \left\| \mathbf{h}_k^T \mathbf{W} \right\|_2^2 + \tilde{\sigma}_k^2} = \frac{\mathbf{w}^H \mathbf{B}_k \mathbf{w}}{\mathbf{w}^H \mathbf{G}_k + \tilde{\sigma}_k^2} \tag{5}$$

where $\mathbf{B}_k = P_{\bar{k}}(\mathbf{h}_k^T \odot \mathbf{h}_{\bar{k}}^T)^H(\mathbf{h}_k \odot \mathbf{h}_{\bar{k}})^T$ and $\mathbf{G}_k = \sigma^2(\text{diag}(\mathbf{h}_k))^H\text{diag}(\mathbf{h}_k)$.

3.3 Energy Consumption at Relays

We consider a practical power amplifier model whose efficiency depends on the output power [25]. In particular, we define $\widetilde{\mathbf{Q}} = P_1(\text{diag}(\mathbf{h}_1))^H\text{diag}(\mathbf{h}_1) + P_2(\text{diag}(\mathbf{h}_2))^H\text{diag}(\mathbf{h}_2) + \sigma^2\mathbf{I}_L$, $\mathbf{e}_l \triangleq [\underset{l-1}{0,\ldots,0}, 1, \underset{L-l}{0,\ldots,0}]$ and $\mathbf{Q}_l = \text{diag}(\mathbf{e}_l)\widetilde{\mathbf{Q}}$.

Then, the radiated power at relay l is $\mathbf{w}^H\mathbf{Q}\mathbf{w}$. The amplifier efficiency at relay l is

$$\epsilon_l(\mathbf{w}) = \frac{\hat{\epsilon}_l}{\hat{P}_l}\sqrt{\mathbf{w}^H\mathbf{Q}_l\mathbf{w}} \tag{6}$$

where $\hat{\epsilon}_l$ and $\hat{P}_l$ are maximum efficiency and maximum power outputted by the amplifier. The power consumed by the amplifier at relay l is

$$P_l^{\text{amp}}(\mathbf{w}) = \frac{\mathbf{w}^H\mathbf{Q}_l\mathbf{w}}{\epsilon_l(\mathbf{w})} = \alpha_l\sqrt{\mathbf{w}^H\mathbf{Q}_l\mathbf{w}} \tag{7}$$

where $\alpha_l = \frac{\hat{P}_l}{\hat{\epsilon}_l}$. On the other hand, other functions of the relays also need energy for operating. Let E_l^c denote the consumed circuit energy at relay l which is constant [26]. Clearly, the relays successfully assist the information transmission if the consumed energy does not exceed the harvested one, i.e.,

$$\frac{(1-\tau)T}{2}P_l^{\text{amp}}(\mathbf{w}) + E_l^c \leq E_l(\tau) \tag{8}$$

3.4 Sum-Rate Maximization Problem

We aim at jointly designing processing vector w and time fraction τ such that the total transmitted data in the system is maximized. Mathematically, the problem is formulated as

$$\underset{\mathbf{w},\tau}{\text{maximize}} \quad \sum_{k=1,2} R_k(\mathbf{w},\tau) \tag{9a}$$

$$\text{subject to} \quad \frac{(1-\tau)T}{2}P_l^{\text{amp}}(\mathbf{w}) + E_l^c \leq E_l(\tau), \forall l = 1,\ldots,L \tag{9b}$$

where $R_k(\mathbf{w},\tau) \triangleq \frac{(1-\tau)T}{2}\log(1+\gamma_k)$ is the data rate transmitted by user k . Problem (9) is highly nontrackable since both the objective function and feasible set are nonconvex. In the following, we present an efficient low-complexity algorithm solving (9) locally.

4 PROPOSED ALGORITHM

We develop the proposed algorithm based on the Majorization-minimization (MM) technique, which has been widely used in wireless communication designs for tackling nonconvex problems [27]. The core idea is to obtain convex approximate problems of the nonconvex problem by replacing the nonconvex parts with proper convex surrogates. For this purpose, we first rewrite (9) in a simpler formulation given as

$$\underset{\mathbf{w},0<\tau<1}{\text{maximize}} \quad \sum_{k=1,2}(1-\tau)\log\left(1+\frac{\mathbf{w}^H\mathbf{B}_k\mathbf{w}}{\mathbf{w}^H\mathbf{G}_k\mathbf{w}+\tilde{\sigma}_k^2}\right) \tag{10a}$$

$$\text{subject to} \quad \sqrt{\mathbf{w}^H\mathbf{Q}_l\mathbf{w}}+\bar{\mathrm{A}}_l \le \frac{F_l}{1-\tau}, \forall l=1,\ldots,L \tag{10b}$$

where $\bar{\mathrm{A}}_l = 2A_l \,/\, \alpha_l$ and $F_l = \bar{\mathrm{A}}_l - 2E_l^c \,/\, (\alpha_l T)$.

Equivalence Transformation

We observe that the objective in (10) is still complex due to the SINR terms. Towards a formulation amenable to MM technique, we introduce slack variables $\mathbf{v} \triangleq \{v_k\}_k$ and $\boldsymbol{\mu} \triangleq \{\mu_k\}_k$, then translate (10) into the following problem

$$\underset{\substack{\boldsymbol{w},0<\tau<1,\\ \mathbf{v}>0,\boldsymbol{\mu}>0}}{\text{maximize}} \quad (1-\tau)(\mu_1+\mu_2) \tag{11a}$$

$$\text{subject to} \quad \mathbf{w}^H\mathbf{G}_k\mathbf{w}+\tilde{\sigma}_k^2 \le \frac{\mathbf{w}^H\mathbf{B}_k\mathbf{w}}{v_k}, k=1,2 \tag{11b}$$

$$\mu_k \le \log(1+v_k), k=1,2 \tag{11c}$$

$$\sqrt{\mathbf{w}^H\mathbf{Q}_l\mathbf{w}}+\bar{\mathrm{A}}_l \le \frac{F_l}{1-\tau}, \forall l=1,\ldots,L. \tag{11d}$$

Here constraints (11b) and (11c) are active at the optimal solutions. To see this, let us suppose that there exists an optimal point $(\boldsymbol{w}^*, \tau^*, \mathbf{v}^*, \boldsymbol{\mu}^*)$ such that (11b) is inactive. Then we can always find $v_k' > 0$ and $\mu_k' > 0$ such that the point $(\mathbf{w}^*, \tau^*, \{v_k^* + v_k'\}_k, \{\mu_k^* + \mu_k'\}_k)$ is feasible and $(1-\tau^*)(\mu_1^*+\mu_2^*) < (1-\tau^*)(\mu_1^*+\mu_1'+\mu_2^*+\mu_2')$. This contradicts the assumption that $(\boldsymbol{w}^*, \tau^*, \mathbf{v}^*, \boldsymbol{\mu}^*)$ is optimal. The fact means (10) and (11) are optimally equivalent.

It is worth noting that the MM technique can be directly applied to solve (11). Specifically, we remark that the objective has a convex representation due to the fact the hyperbolic constraint $xy \ge z^2$, where $x > 0$ and $y > 0$, can be converted to second-order cone one given as $||[2z\ x-y]||_2 \le x+y$. On the other hand, the nonconvex constraint (11b) and (11d) are in the difference-of-convex (DoC) form. Thus, we can use first-order the Taylor series to derive their valid convex surrogates.

Alternatively, we present a simple transformation of (11) where only one type of constraints will be approximated. In particular, let us make a simple variable change $\hat{\tau} = \frac{1}{1-\tau}$ which turns (11d) convex, i.e. (11) is equivalent to

$$\underset{\substack{\widehat{\mathbf{w}},\hat{\tau}>0,\\ \mathbf{v}>0,\boldsymbol{\mu}>0}}{\text{maximize}} \quad \frac{(\mu_1+\mu_2)}{\hat{\tau}} \tag{12a}$$

$$\text{subject to} \quad \sqrt{\mathbf{w}^H\mathbf{Q}_l\mathbf{w}} + \bar{\mathrm{A}}_l \le F_l\hat{\tau}, \forall l = 1,\ldots,L. \tag{12b}$$

$$(11b),(11c). \tag{12c}$$

Now by applying the Charnes Cooper transformation to (12), we arrive at the following problem

$$\underset{\substack{\widetilde{\mathbf{w}},\xi>0\\ \tilde{\mathbf{v}}>0,\tilde{\boldsymbol{\mu}}>0}}{\text{maximize}} \quad (\tilde{\mu}_1 + \tilde{\mu}_2) \tag{13a}$$

$$\text{subject to} \quad \frac{\widetilde{\boldsymbol{w}}^H\mathbf{G}_k\widetilde{\boldsymbol{w}}}{\xi} + \xi\tilde{\sigma}_k^2 \le \frac{\widetilde{\mathbf{w}}^H\mathbf{B}_k\widetilde{\mathbf{w}}}{\tilde{v}_k}, k = 1,2 \tag{13b}$$

$$\tilde{\mu}_k \le \xi\log(1+\tfrac{\tilde{v}_k}{\xi}), k = 1,2 \tag{13c}$$

$$\sqrt{\widetilde{\mathbf{w}}^H\mathbf{Q}_l\widetilde{\mathbf{w}}} + \xi\bar{\mathrm{A}}_l \le F_l, \forall l = 1,\ldots,L \tag{13d}$$

where $\tilde{\mathbf{v}} \triangleq \{\tilde{v}_k\}_k$ and $\tilde{\boldsymbol{\mu}} \triangleq \{\tilde{\mu}_k\}_k$

Theorem 1. *Let* $(\widetilde{\mathbf{w}}, \xi, \tilde{\mathbf{v}}, \tilde{\boldsymbol{\mu}})$ *be an optimal solution of (13), then* $(\frac{\widetilde{\mathbf{w}}}{\xi}, \frac{1}{\xi}, \frac{\tilde{\mathbf{v}}}{\xi}, \frac{\tilde{\boldsymbol{\mu}}}{\xi})$ *is an optimal solution of (12). Reversely, let* $(w, \hat{\tau}, v, \mu)$ *be an optimal solution of (12), then* $(\frac{\boldsymbol{w}}{\hat{\tau}}, \frac{1}{\hat{\tau}}, \frac{\mathbf{v}}{\hat{\tau}}, \frac{\boldsymbol{\mu}}{\hat{\tau}})$ *is an optimal solution of (13).*

The theorem encourages us to focus on solving (13), since here only (13b) causes (13) nonconvex. Constraint (13b) is in DoC form. Thus its valid convex surrogate can be achieved via first-order Taylor series as

$$\frac{\widetilde{\mathbf{w}}^H\mathbf{G}_k\widetilde{\mathbf{w}}}{\xi} + \tilde{\sigma}_k^2 \;\le\; \frac{2\Re\{(\widetilde{\mathbf{w}}^{(i)})^H\boldsymbol{B}_k\widetilde{\mathbf{w}}\}}{\tilde{v}_k^{(i)}} - \frac{(\widetilde{\mathbf{w}}^{(i)})^H\boldsymbol{B}_k\widetilde{\mathbf{w}}^{(i)}}{\left(\tilde{v}_k^{(i)}\right)^2}\tilde{v}_k, k = 1,2 \tag{14}$$

where $(\widetilde{\mathbf{w}}^{(i)}, \xi^{(i)}, \tilde{\mathbf{v}}^{(i)}, \tilde{\boldsymbol{\mu}}^{(i)})$ is a feasible point. Then, a convex approximate of (13) is

$$\underset{\substack{\widetilde{\mathbf{w}},\xi>0\\ \tilde{\mathbf{v}}>0,\tilde{\boldsymbol{\mu}}>0}}{\text{maximize}} \quad (\tilde{\mu}_1 + \tilde{\mu}_2) \;\; \text{subject to (13c),(13d),(14).} \tag{15}$$

The proposed algorithm is an iterative procedure outlined in Algorithm 1. In each iteration, a convex approximate problem is solved (Step 3) and the feasible point is updated (Step 4). It is worth remarking that Algorithm 1 inherits the convergence properties of the MM framework. In particular, the sequence $\left\{(\tilde{\mu}_1^{(i)} + \tilde{\mu}_2^{(i)})\right\}_{i=0}^{\infty}$ is nondecreasing, and the convergence points satisfy the Karush–Kuhn–Tucker conditions of (13).

Algorithm 1 The proposed iterative procedure for solving (9)

1: **Initialization**: Set i := 0, and generate a feasible point $(\widetilde{\mathbf{w}}^{(i)}, \xi^{(i)}, \tilde{\mathbf{v}}^{(i)}, \tilde{\boldsymbol{\mu}}^{(i)})$.
2: **repeat**
3: Determine the optimal solution of (15), denoted by $(\boldsymbol{w}^*, \xi^*, \mathbf{v}^*, \boldsymbol{\mu}^*)$.
4: Set i := i + 1 and $(\widetilde{\mathbf{w}}^{(i)}, \xi^{(i)}, \widetilde{\boldsymbol{v}}^{(i)}, \tilde{\boldsymbol{\mu}}^{(i)}) := (\boldsymbol{w}^*, \xi^*, \mathbf{v}^*, \boldsymbol{\mu}^*)$.
5: **until** Convergence criteria is satisfied
6: **Output**: $(\frac{\widetilde{\mathbf{w}}^{(i)}}{\xi^{(i)}}, 1 - \xi^{(i)})$

5 SELF-INTERFERENCE SUPPRESSION

Up to now, the self-interference is supposed to be perfectly subtracted at the users prior to decoding. However, self-interference cancellation may require additional signaling overhead in practice [28]. In this section, we relax this assumption and present two schemes overcoming the self-interference issue.

5.1 Scheme 1

In the first scheme user k decodes information based on $\tilde{y}_k$ and treat the self-interference as additional noise. Specifically, the SINR at user k is given by

$$\gamma_k = \frac{P_{\bar{k}}|\boldsymbol{h}_k^T \boldsymbol{W} \boldsymbol{h}_{\bar{k}}|^2}{P_k|\boldsymbol{h}_k^T \boldsymbol{W} \boldsymbol{h}_k|^2 + \sigma^2||\boldsymbol{h}_k^T \boldsymbol{W}||_2^2 + \tilde{\sigma}_k^2} = \frac{\boldsymbol{w}^H \boldsymbol{B}_k \boldsymbol{w}}{\boldsymbol{w}^H (\boldsymbol{S}_k + \boldsymbol{G}_k)\boldsymbol{w} + \tilde{\sigma}_k^2} \tag{16}$$

where $S_k = P_k(\mathbf{h}_k^T \odot \mathbf{h}_k^T)^H(\mathbf{h}_k \odot \mathbf{h}_k)^T$.

Then the problem of sum rate maximization can be written as

$$\underset{\mathbf{w}, 0<\tau<1}{\text{maximize}} \quad \sum_{k=1,2} (1-\tau) \log\left(1 + \frac{\mathbf{w}^H \mathbf{B}_k \mathbf{w}}{\mathbf{w}^H (\mathbf{S}_k + \mathbf{G}_k)\boldsymbol{w} + \tilde{\sigma}_k^2}\right) \tag{17a}$$

$$\text{subject to} \quad \sqrt{\mathbf{w}^H \mathbf{Q}_l \mathbf{w}} + \bar{A}_l \leq \frac{F_l}{1-\tau}, \forall l = 1,\ldots,L. \tag{17b}$$

The problem is in a similar form of (10) and thus can be solved by an iterative procedure similar to Algorithm 1.

5.2 Scheme 2

In the second scheme, the beamforming vector w is designed based on the null-space beamforming technique which eliminates the self-interference. Towards the goal, let us introduce the matrix $\mathbf{H} = [(\mathbf{h}_1 \odot \mathbf{h}_1), (\mathbf{h}_2 \odot \mathbf{h}_2)]^T \in \mathbb{C}^{2\times L}$. Then we have

$$\boldsymbol{h}_k^T \boldsymbol{W} \boldsymbol{h}_k = 0 \text{ for } k = \{1,2\} \Leftrightarrow \boldsymbol{H}\boldsymbol{w} = 0 \tag{18}$$

Which can be satisfied by constructing $\mathbf{w}$ as follows. Let us denote by $\mathbf{D} \in \mathbb{C}^{L\times(L-2)}$ an orthogonal basis of null-space of $\mathbf{H}$, which exists when $L > 2$. Then the beamforming vector is constructed as $\mathbf{w} = \mathbf{D}\mathbf{m}$ where $\mathbf{m} \in \mathbb{C}^{(L-2)\times 1}$. Now, let $\widehat{\mathbf{B}}_k = \mathbf{D}^H \mathbf{B}_k \mathbf{D}$, $\widehat{\mathbf{G}}_k = \mathbf{D}^H \mathbf{G}_k \mathbf{D}$, and $\widehat{\mathbf{Q}}_l = \mathbf{D}^H \mathbf{Q}_l \mathbf{D}$, then the sum-rate maximization problem becomes

$$\underset{\mathbf{m}, 0<\tau<1}{\text{maximize}} \quad \sum_{k=1,2} (1-\tau) \log\left(1 + \frac{\mathbf{m}^H \widehat{\mathbf{B}}_k \mathbf{m}}{\mathbf{m}^H \widehat{\mathbf{G}}_k \mathbf{m} + \sigma_k^2}\right) \tag{19a}$$

$$\text{subject to} \quad \sqrt{\mathbf{m}^H \widehat{\mathbf{Q}}_l \mathbf{m}} + \bar{A}_l \leq \frac{F_l}{1-\tau}, \forall l = 1,\ldots,L. \tag{19b}$$

Again, a procedure similar to Algorithm 1 can be used to achieve solutions of (19).

6 NUMERICAL ANALYSIS

We now numerically evaluate the proposed schemes. We consider a simulation system model based on those in [14]-[16]. Specifically, the channel coefficients are generated as $h_{kl} = d_{kl}^{-3/2}\bar{h}_{kl}$ where d_{kl} is the distance between user k and relay l, which is generated randomly between 4m and 6m, and $\bar{h}_{kl} \backsim CN(0,1)$. The noise variances are simply set as $\tilde{\sigma}_k^2 = \sigma^2 = -43$ dBm. The system bandwidth is 1 MHz. For the EH parameters we set $a_l = 150$, $b_l = 0.014$, $\bar{P}_l = 24$ mW. For the power amplifier model, we take $\hat{\varepsilon}_l = 0.55$ and $\hat{P}_l = 33$ dBm. The consumed circuit energy is $E_l^c = 3.5$ mJoule. Without loss of generality, let $T = 1$ second for simplicity. All the convex problems are solved by the modeling package CVX with internal solver SDPT3 [29].

For starting Algorithm 1, we merely generate an initial point $(\widetilde{\mathbf{w}}^{(0)}, \xi^{(0)}, \tilde{\mathbf{v}}^{(0)}, \widetilde{\boldsymbol{\mu}}^{(0)})$ as follows. First, we randomly generate a point $(\mathbf{w}^{(0)}, \tau^{(0)})$ and scale it (if necessary) so that (9b) is satisfied. Then, we determine $\mathbf{v}^{(0)}$ and $\boldsymbol{\mu}^{(0)}$ by letting (11b) and (11c) be at equality, respectively. Finally, we set $\widetilde{\mathbf{w}}^{(0)} = (1-\tau^{(0)})\mathbf{w}^{(0)}$, $\xi^{(0)} = (1-\tau^{(0)})$, $\tilde{\mathbf{v}}^{(0)} = (1-\tau^{(0)})\mathbf{v}^{(0)}$ and $\widetilde{\boldsymbol{\mu}}^{(0)} = (1-\tau^{(0)})\boldsymbol{\mu}^{(0)}$.

We also consider the scheme in [15] as the baseline for evaluating our schemes. We recall that [15] did not consider the practical models of energy harvester and power amplifier. Thus, a mapping step is required. In particular, we run the method in [15] with the ideal models of energy harvester and power amplifier and obtain a solution $(\mathbf{w}', \tau')$. Then we simply scale $\mathbf{w}'$ (if necessary) such that (9b) is satisfied. Finally, the sum rate is calculated with this (scaled) point.

For the convergence criteria, all the considered iterative procedures stop when the increase in the objective of the two successive iterations is less than 10^{-4}. We investigate the convergence performance of Algorithm 1. In Figure 10, the results of cumulative distribution function comparison clearly shows that the CDF required from 13 to 15 of iterations to converge in our own proposed algorithm.

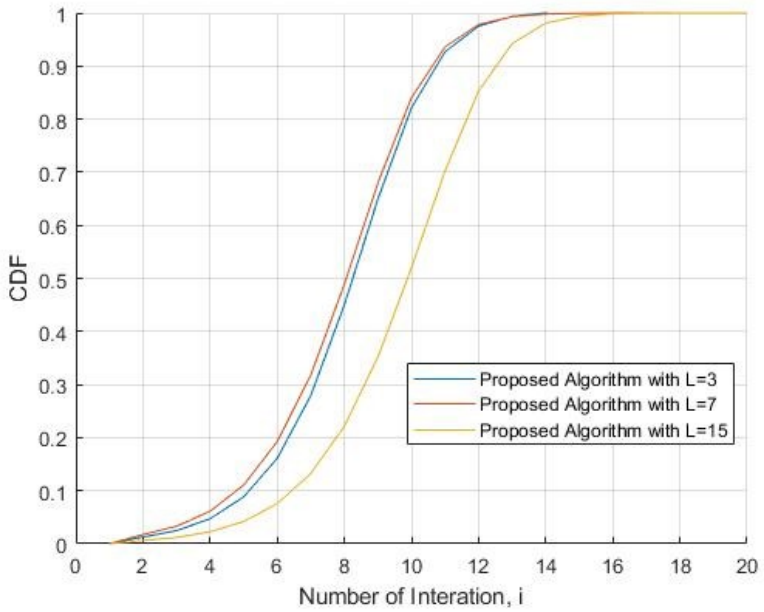

Figure 10 Cumulative Distribution Function.

In [15], the authors design a resources allocation algorithm for the two-way relaying network based on the linear EH model. We want to compare the maximum sum-rate performance between our own non-linear model and their linear model. The comparison result is shown in Figure 11. There are significantly sum-rate performance improvement in the non-linear model compared its performance with a linear model. More importantly, the non-linear assumption for the EH receiver model does follow the actual characterization of practical EH circuits in practice.

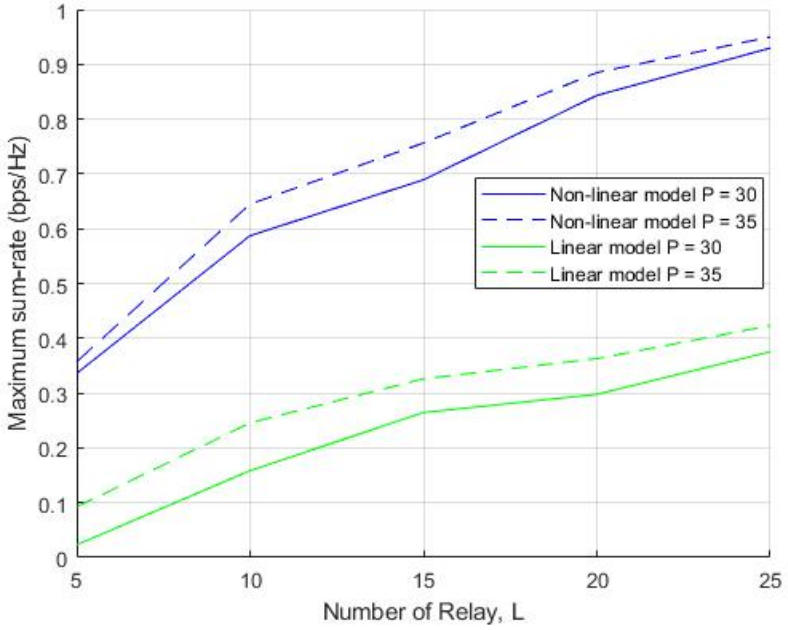

Figure 11 Comparison between the non-linear model and the linear model

In Figure 12, we compare the proposed algorithm with a different value of power transmission. There is slightly better performance at higher power with a small number of the RSs. The performance is not much different with a large number of the RSs.

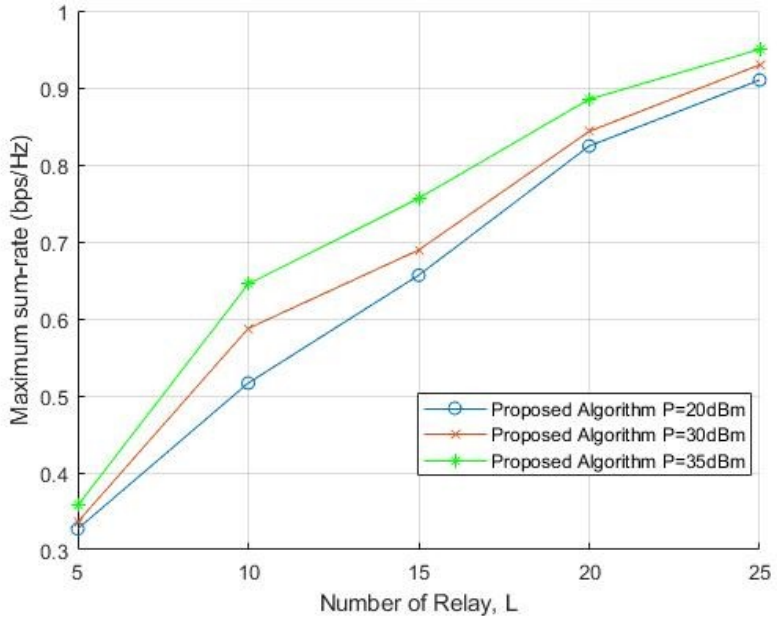

Figure 12. The maximum sum-rate performance with the proposed algorithm and P=20,30,35.

In Figure 13, the comparison in maximum sum-rate performance between the proposed algorithm with interference-free and interferences suppression Scheme 1 and Scheme 2 in another case. It is also demonstrating how the proposed algorithm benefits from increasing the number of the relay station. Both schemes illustrate a great performance compare to the interference-free sum-rate performance. Scheme 2 shown slightly better sum-rate with some relay station support. However, both schemes achieve approximately the same rate with a massive number of relay station support.

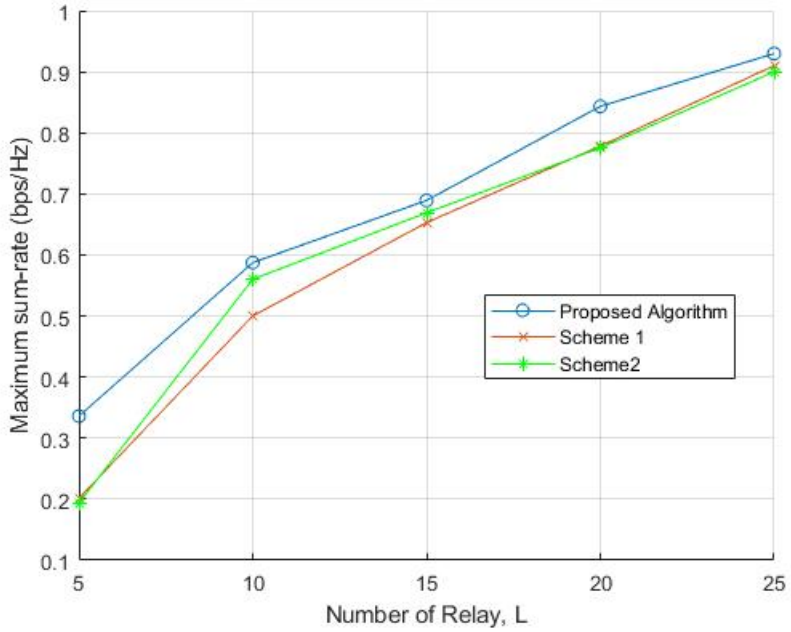

Figure 13 Performance comparison between the proposed algorithm, scheme 1 and scheme 2.

Maximum sum-rate versus the time allocation factor in three different scenarios shown in Figure 14. It is clearly shown that the best τ value equal to 0.2 in order to get the best sum-rate maximum performance. Furthermore, our suppression scheme shown a really good performance to deal with interference, especially in AF technology which is easier to get bad influence by strong interference signal.

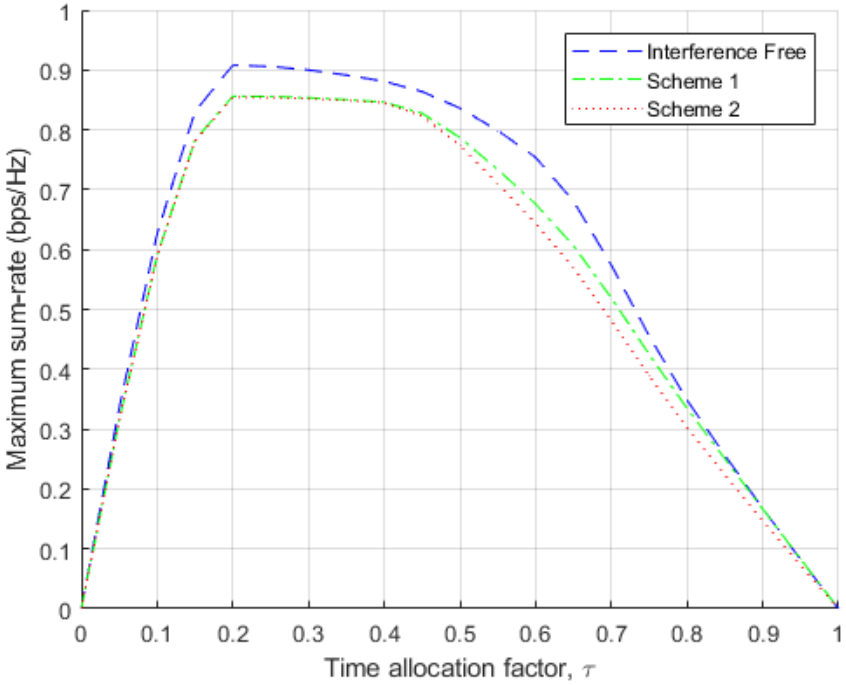

Figure 14 Maximum sum-rate versus the time allocation factor in three different scenarios.

7 DISCUSSION

There is still discussion between the non-linear model and the linear model in energy harvesting system. The result of our experiment shown that the linear assumption for the EH receiver model does not follow the actual characterization of practical EH circuits. In practice, the parameters of the EH circuits are non-linear. The result showed significant performance losses in SWIPT systems, when the design of the resource allocation algorithm is based on an inaccurate linear EH model.

In the future work, we tend to use the practical non-linear EH receiver model for designing resource allocation algorithms in different variations of SWIPT systems, for example harvesting energy system with imperfect CSI. Moreover, we are interested in investigating the possible performance gain of the proposed model in different concepts with EH.

The distributed beamforming is considering in a simple two-way relaying network with a single antenna. In practice, beamforming enables distributed energy sources to cooperate with an antenna array by transmitting RF energy simultaneously in the same direction to an intended harvester node for better diversity gains. The results expected to has sustainably gain more energy as the same as energy gain from the full knowledge information beamforming. The challenges begin in the implementation phase such as time synchronization among energy sources and coordination of distributed carriers in phase and frequency so that RF signals can be combined constructively at the receiver need to take into account.

Interference management technique also needs development in order to achieve the best SWIPT system performance. For example, the SWIPT system with RF energy harvesting can turn harmful interference into useful energy through a scheduling policy. Therefore, mitigate interference as well as promote energy transfer is the problem to be addressed. Moreover, the scheduling policy combined with power management schemes might be an excellent solution for improvement in energy efficiency.

8 SUMMARY

The thesis focuses on the analysis and optimization of various energy constrained in the energy harvesting system. The typical two-way relay system is taking into account in this thesis simulation. We propose a new algorithm and study the best time allocation factor for the two-way relay network to achieve the maximum sum-rate performance.

Furthermore, we apply some suppression scheme to solving the interference issues. In the most existing study consider ideal assumptions when studying the SWIPT system. In this thesis, we are also assuming the interference, and we deploy two different schemes to suppression interference to see the influence of it in sum-rate performance.

Furthermore, we solve the nonconvex problem by MM technique to achieve the best time allocation factor to maximize the sum-rate of the system. The best time allocation factor can be achieved to maximum sum-rate performance. The time allocation factor might have a different value in another case because it depends on a distance of node set in the simulation. When the distance is set with a different value, the time allocation factor will change. The result shows that the proposed algorithm is performing tremendously well and achieves close to optimal in an interference-free environment with a massive number of relay station supporting. CDF required from 13 to 15 of iterations to converge in own proposed algorithm.

In practice, the parameters of the EH circuits are non-linear; hence, the wireless power transfer model needs to follow the non-linear model to design the practical EH system. Moreover, the result showed significant performance losses in SWIPT systems, when the design of the resource allocation algorithm is based on an inaccurate linear EH model. As the result, the non-linear model must be used for harvesting energy in the SWIPT system.

Lastly, power transmission and the number of RSs are both crucial factors affecting sum-rate performance. However, the sum-rate performance is generally the same with a high number of RS. In the non-interference case, we deployed the suppression interference schemes which are also showing good performance. Both schemes illustrate a great performance comparing with the interference-free sum-rate performance. Scheme 1 shows slightly better sum-rate with a small number of relay station support. However, both schemes achieve approximately the same rate with a massive number of RS.

9 REFERENCES

[1] Bi, S., Ho, C. K., & Zhang, R. (2015). Wireless powered communication: Opportunities and challenges. IEEE Communications Magazine, 53(4), 117-125.

[2] Krikidis, I., Timotheou, S., Nikolaou, S., Zheng, G., Ng, D. W. K., & Schober, R. (2014). Simultaneous wireless information and power transfer in modern communication systems. IEEE Communications Magazine, 52(11), 104-110.

[3] Xie, L., Shi, Y., Hou, Y. T., & Lou, A. (2013). Wireless power transfer and applications to sensor networks. IEEE Wireless Communications, 20(4), 140-145.

[4] Lu, X., Wang, P., Niyato, D., Kim, D. I., & Han, Z. (2015). Wireless networks with RF energy harvesting: A contemporary survey. IEEE Communications Surveys & Tutorials, 17(2), 757-789.

[5] Zhang, R., & Ho, C. K. (2013). MIMO broadcasting for simultaneous wireless information and power transfer. IEEE Transactions on Wireless Communications, 12(5), 1989-2001.

[6] Ding, Z., Zhong, C., Ng, D. W. K., Peng, M., Suraweera, H. A., Schober, R., & Poor, H. V. (2015). Application of smart antenna technologies in simultaneous wireless information and power transfer. IEEE Communications Magazine, 53(4), 86-93.

[7] Ulukus, S., Yener, A., Erkip, E., Simeone, O., Zorzi, M., Grover, P., & Huang, K. (2015). Energy harvesting wireless communications: A review of recent advances. IEEE Journal on Selected Areas in Communications, 33(3), 360-381.

[8] Nasir, A. A., Zhou, X., Durrani, S., & Kennedy, R. A. (2013). Relaying protocols for wireless energy harvesting and information processing. IEEE Transactions on Wireless Communications, 12(7), 3622-3636.

[9] Ding, Z., Perlaza, S. M., Esnaola, I., & Poor, H. V. (2014). Power allocation strategies in energy harvesting wireless cooperative networks. IEEE Transactions on Wireless Communications, 13(2), 846-860.

[10] Dong, M., & Shahbazpanahi, S. (2010, March). Optimal spectrum sharing and power allocation for OFDM-based two-way relaying. In Acoustics Speech and Signal Processing (ICASSP), 2010 IEEE International Conference on (pp. 3310-3313). IEEE.

[11] Papotto, G., Carrara, F., Finocchiaro, A., & Palmisano, G. (2014). A 90-nm CMOS 5-Mbps crystal-less RF-powered transceiver for wireless sensor network nodes. IEEE Journal of Solid-State Circuits, 49(2), 335-346.

[12] Gurakan, B., Ozel, O., Yang, J., & Ulukus, S. (2012, July). Energy cooperation in energy harvesting wireless communications. In Information Theory Proceedings (ISIT), 2012 IEEE International Symposium on (pp. 965-969). IEEE.

[13] Ulukus, S., Yener, A., Erkip, E., Simeone, O., Zorzi, M., Grover, P., & Huang, K. (2015). Energy harvesting wireless communications: A review of recent advances. IEEE Journal on Selected Areas in Communications, 33(3), 360-381.

[14] Weddell, A. S., Magno, M., Merrett, G. V., Brunelli, D., Al-Hashimi, B. M., & Benini, L. (2013, March). A survey of multi-source energy harvesting systems. In Design, Automation & Test in Europe Conference & Exhibition (DATE), 2013 (pp. 905-908). IEEE.

[15] Salari, S., Kim, I. M., Kim, D. I., & Chan, F. (2017). Joint EH time allocation and distributed beamforming in interference-limited two-way networks with EH-based relays. IEEE Transactions on Wireless Communications, 16(10), 6395-6408.

[16] Havary-Nassab, V., Shahbazpanahi, S., & Grami, A. (2010). Optimal distributed beamforming for two-way relay networks. IEEE Transactions on Signal Processing, 58(3), 1238-1250.

[17] Koike-Akino, T., Popovski, P., & Tarokh, V. (2009). Optimized constellations for two-way wireless relaying with physical network coding. IEEE Journal on Selected Areas in Communications, 27(5).

[18] Zhang, R., Liang, Y. C., Chai, C. C., & Cui, S. (2009). Optimal beamforming for two-way multi-antenna relay channel with analogue network coding. IEEE Journal on Selected Areas in Communications, 27(5).

[19] Wu, Y., Chou, P. A., & Kung, S. Y. (2005). Information exchange in wireless networks with network coding and physical-layer broadcast (Vol. 78). MSR-TR-2004.

[20] Hammerstrom, I., Kuhn, M., Esli, C., Zhao, J., Wittneben, A., & Bauch, G. (2007, June). MIMO two-way relaying with transmit CSI at the relay. In Signal processing advances in wireless communications, 2007. SPAWC 2007. IEEE 8th Workshop on(pp. 1-5). IEEE.

[21] Yuen, C., Chin, W. H., Guan, Y. L., Chen, W., & Tee, T. (2008, May). Bi-directional multi-antenna relay communications with wireless network coding. In Vehicular Technology Conference, 2008. VTC Spring 2008. IEEE (pp. 1385-1388). IEEE.

[22] E. Boshkovska, D. W. K. Ng, N. Zlatanov, and R. Schober, “Practical non-linear energy harvesting model and resource allocation for SWIPT systems,” IEEE Commun. Lett., vol. 19, no. 12, pp. 2082–2085, Dec 2015

[23] Boshkovska, E., Morsi, R., Ng, D. W. K., & Schober, R. (2016, May). Power allocation and scheduling for SWIPT systems with non-linear energy harvesting model. In 2016 IEEE International Conference on Communications (ICC) (pp. 1-6). IEEE.

[24] Rankov, B., & Wittneben, A. (2007). Spectral efficient protocols for half-duplex fading relay channels. IEEE Journal on Selected Areas in Communications, 25(2). Chicago.

[25] Persson, D., Eriksson, T., & Larsson, E. G. (2013). Amplifier-aware multiple-input multiple-output power allocation. IEEE Communications Letters, 17(6), 1112-1115.

[26] Auer, G., Giannini, V., Desset, C., Godor, I., Skillermark, P., Olsson, M., ... & Fehske, A. (2011). How much energy is needed to run a wireless network?. IEEE Wireless Communications, 18(5).

[27] Sun, Y., Babu, P., & Palomar, D. P. (2017). Majorization-minimization algorithms in signal processing, communications, and machine learning. IEEE Transactions on Signal Processing, 65(3), 794-816.

[28] Yemini, M., Zappone, A., Jorswieck, E., & Leshem, A. (2017). Energy efficient bidirectional massive MIMO relay beamforming. IEEE Signal Processing Letters, 24(7), 1010-1014.

[29] M. Grant and S. Boyd, “CVX: Matlab software for disciplined convex programming, version 2.0 beta,” http://cvxr.com/cvx, Sep. 2012.